Respuestas, 25 (3), September-December 2020, pp. 54-78, ISSN 0122-820X - E ISSN: 2422-5053

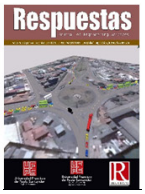

Respuestas
Journal of Engineering Sciences
RESPUESTAS

Original Article https://doi.org/10.22463/0122820X.2707

Technical-economic analysis of [Bmim][BF4] for the post-combustion CO2 capture at "Termocentro" thermoelectric plant, Colombia

Análisis Técnico-económico de [Bmim][BF4] para la captura de CO2 de post-combustion de la planta termoeléctrica de "Termocentro"

Walter David Sanchez-Peinado[1], Eliseo Amado-González[2*], Edwin Gustavo Fuentes-Ordóñez[3]

[1]*Ingeniero Químico, walter.sanchez@unipamplona.edu.co, ORCID: 0000-0002-1862-4386, University of Pamplona, Pamplona, Colombia.*
[2*]*Doctor en Ciencias Química, eamado@unipamplona.edu.co, ORCID: 0000-0003-4523-1323, University of Pamplona, Pamplona, Colombia.*
[3]*Doctor en Ingeniería Química, efuenteso@unicartagena.edu.co, ORCID: 0000-0001-5365-1059, University of Cartagena, Cartagena, Colombia.*

How to cite: W. D. Sanchez-Peinado, E. Amado-González, E. G Fuentes-Ordóñez, "Technical-economic analysis of [Bmim][BF4] for the post-combustion CO2 capture at "Termocentro" thermoelectric plant, Colombia". *Respuestas,* vol. 25, no. 2, pp. 54-78, 2020.

Received on June 22, 2020 - Approved on October 23, 2020.

ABSTRACT

Keywords:

Carbon dioxide,
ionic liquid,
Monoethanolamine,
Simulation,
Aspen Plus

In the present work, steady-state simulations of the natural gas combined cycle (NGCC) and the post-combustion CO2 capture (PCC) processes have been modeled in the Aspen Plus® environment. The capture plan model was validated with data from the Colombian power plant "Termocentro" at 300MWe. A techno-economical evaluation study has been performed for both a combined cycle (gas and steam) and the PCC process. The PCC process was based on the solvent 30% (w/w) MEA-H2O and on the solvent H2O-30% (w/w)-MEA-5% (w/w))-[Bmim][Bf4]. Sensitivity analysis was carried out, giving, as a result, an optimum concentration of 5% (w/w) for the 1-butyl-3-methylimidazolium tetrafluoroborate ionic liquid ([Bmim][BF4]) solvent. The study indicates how with efficient operation conditions of solvent regeneration, [Bmim][Bf4] may be used for CO2 capture plans in the future.

RESUMEN

Palabras clave:

Dioxido de carbon,
líquido iónico,
etanolamina,
simulación,
Aspen Plus

En el presente trabajo, las simulaciones de estado estacionario del ciclo combinado de gas natural (NGCC) y los procesos de captura de CO2 poscombustión (PCC) se han modelado en el entorno Aspen Plus®. El modelo del plan de captura fue validado con datos de la central colombiana "Termocentro" a 300MWe. Se ha realizado un estudio de evaluación tecno-económico tanto para un ciclo combinado (gas y vapor) como para el proceso PCC. El proceso de PCC se basó en el disolvente 30% (p / p) MEA-H2O y en el disolvente H2O-30% (p / p) -MEA-5% (p / p)) - [Bmim] [Bf4]. Se llevó a cabo un análisis de sensibilidad, dando como resultado una concentración óptima del 5% (p / p) para el disolvente líquido iónico de tetrafluoroborato de 1-butil-3-metilimidazolio ([Bmim] [BF4]). El estudio indica cómo con condiciones de operación eficientes de regeneración de solventes, [Bmim] [Bf4] puede usarse para planes de captura de CO2 en el futuro.

Introduction

Background and motivations

The Intergovernmental Panel on Climate Change considers that CO2 accounts for 65% of total greenhouse gas (GHG) emissions, being the focus of mitigation technologies for sequestration of CO2 (IPCC, 2014; Kijewska & Bluszcz, 2016). The carbon capture and storage process, CCS (Araújo & de Medeiros, 2017) is a potential solution to climate change, which consists of the separation of CO2 from industrial and energy sources, its transport to a storage place, and its long-term atmosphere isolation.

***Corresponding author.**
E-mail Address:eamado@unipamplona.edu.co (Eliseo Amado-González)

The PCC process is a considerably expensive process with high energy consumption, corrosion of equipment; degradation of the solvent - usually ammonia-based compounds - to potentially dangerous and toxic components, and low CO2 composition in the exhaust gas (10-16%) (L. Liu, Zhao, Deng, & An, 2016; Ramdin, De Loos, & Vlugt, 2012). The aforementioned has prevented the massification of the technology at an industrial level and has led to exhaustive research in the exploration of solutions that reduce these negative factors (Leung, Caramanna, & Maroto-Valer, 2014).

The use of an aqueous MEA solution in the CO2 absorption process is considered a mature technology (Abu-Zahra, Schneiders, Niederer, Feron, & Versteeg, 2007; Davis & Rochelle, 2009).Specifically, a solution of 30%MEA weight is used as a reference solvent for CO2 capture (Abu-Zahra et al., 2007). In a 600 MWe bituminous coal plant effluent gas using Aspen Plus®, to evaluate CO2 capture level, MEA concentration, CO2 lean solvent loading, operating regenerator's pressure and temperature of the solvent, a significant impact on the solvent regeneration energy with a value of 3.9GJ/tonCO2 was found (Canepa & Wang, 2015). A capture plant scaled to process the stack gas from a 427 MWe CCGT plant with data from a pilot plant showed the reliability of a rate-based model with multiple stages for a 250 MWe CCGT plant exhaust gas and the positive effect in the reduction of operational costs of the coal capture process (Luo & Wang, 2017).

Los disolventes químicos de absorción, como las aminas, presentan problemas medioambientales además del alto riesgo de corrosión por los productos de degradación de las aminas y los gases ácidos húmedos [11]. Desde 1999, un grupo de disolventes llamados líquidos iónicos (IL) parece ser bastante prometedor como disolventes químicos ecológicos. Los IL presentan propiedades físicas versátiles debido a características como presión de vapor insignificante, excelentes propiedades dieléctricas, estabilidad térmica y plataforma sintonizable para el desarrollo de compuestos de captura de CO2 para el proceso de postcombustión (Hasib-ur-Rahman, Siaj, & Larachi, 2010; Janković et al., 2019; Krzemień, Więckol-Ryk, Smoliński, Koteras, & Więcław-Solny, 2016).The imidazolium based IL (5% [Bpy][BF4]-30% MEA) showed savings of 15% related to the regeneration energy on the stripper's boiler (3.2GJ/tonCO2) compared to the conventional process. This promising value may be due to the absorber and stripper equilibrium model that may affect the uncertainty in the results, as well as inferiority with respect to using a rate-based model (Zhang et al., 2009). The results of the [Bpy][BF4]-MEA 30% system using a rate-based model at 5-30% IL showed a reduction of the specific boiler's regeneration energy in the ranges 7-9% and 12-27%, compared with the 30% on MEA conventional process (Zacchello, Oko, Wang, & Fethi, 2017). Specifically, the lowest found value was close to 4.13 GJ/ton CO2, which is 1.3 times higher than that found by (Huang, Zhang, Zhang, Dong, & Zhang, 2014) when using the same system. (Ma et al., 2017) found that the energy consumption by using [Bmim][BF4] and [Bmim][PF6] was reduced by 26.7% and 24.8% respectively, with respect to the process based solely MEA. The results were argued to the use of an equilibrium model and pure high-cost ILs by (Huang et al., 2014). (de Riva et al., 2017) studied 8 ionic liquids in different configurations of packings in both columns, pressure and temperature; CAPEX and OPEX indices for the process were also calculated using a rate-based model [13]. Of the cases evaluated, the most optimal is obtained using the ionic liquid [emim][Ntf2] at a pure state, for which they report an OPEX value of 3.07 M€/year and an OPEX of 1.59 M€/year for the absorption column, 3.6M€/year for the compression section and 1.63-4.08 M€/year for the used IL at a price of 20 M€/kgIL. Finally, regeneration energy of 1.4GJ/tonCO2, which is the lowest value with respect to the previously mentioned works.

In this manuscript, we report the simulation of the PCC and NGCC processes of a Colombian electricity generation plant "Termocentro" using a rate-based model based on MEA and the ionic liquid [Bmim][BF4]. An analysis of Q, L/G as a function of either capture level, solvent loading, IL concentration was performed. Furthermore, an economic analysis of the NGCC and PCC processes, in terms of capital and manufacturing costs, and profitability analysis of the PCC process to analyze their economic feasibility throughout time, was done.

Methodology

Simulation of the natural gas combined cycle (NGCC)

The 300 MWe net NGCC thermoelectric power plant (TPW) "Termocentro" of ISAGEN's company with a gas combined cycle (NGCC) plant was selected (ISAGEN, 2018). The TPW has two 1996 Westinghouse W501D5 gas turbines, with a 19 stages axial compressor and four expansion levels where the combustion of the natural gas and compressed air streams occurs.

La energía de los gases de chimenea de las turbinas de gas fue utilizada por un generador de vapor de recuperación de calor (HRSG) para el ciclo de la turbina de vapor, formando el ciclo combinado y produciendo más electricidad. Las turbinas de vapor fueron fabricadas por General Electric, modelo 270T441 1996, con dos sistemas de presión (alta y baja) y flujo de vapor axial. Todas las turbinas están acopladas a generadores trifásicos con aire como medio de ventilación.

The simulation of the Termocentro plant was achieved in Aspen Plus ® environment based on the average composition of the natural gas at different Colombian regions (Guerrero Suarez & Llano Camacho, 2003) (see Figure 1). Both "DESIGN SPEC" and "CALCULATOR" blocks were used to meet the specifications given by (ISAGEN, 2018). A net power output of 100MWe was specified both in each gas turbine by modifying the natural gas flow and a net power output of 100 MWe in each steam turbine was accomplished by varying the gas turbine efficiencies. Airflow varied until 15% in excess concerning the natural gas flow. Water flow was calculated to accomplish a gas outlet temperature in the range of 170-200°C. The gas turbine cooling airflow varied to maintain stack gases temperature at around 530°C.

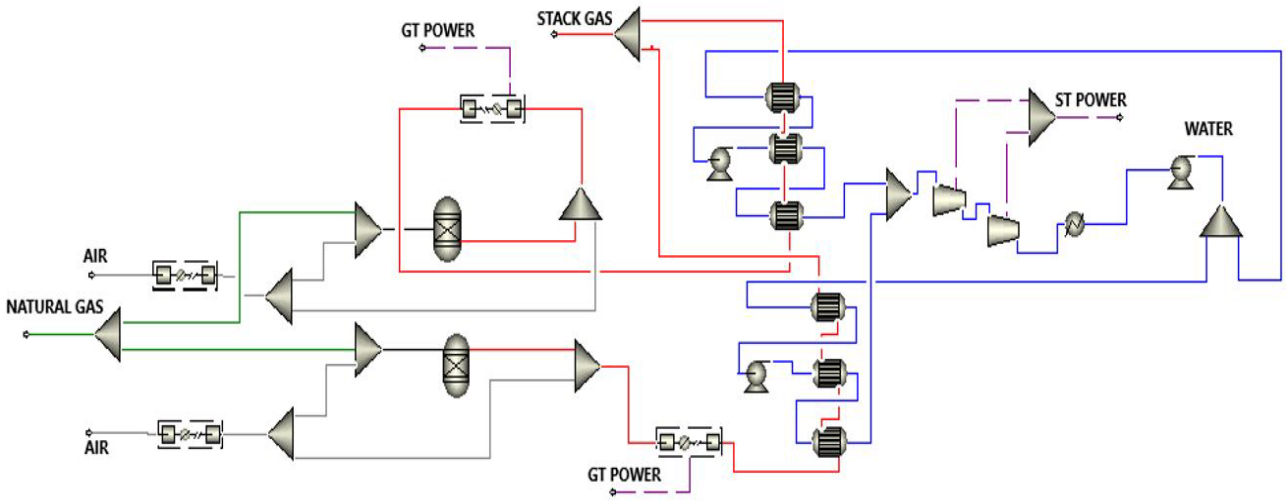

Figure 1. Natural gas combined cycle process flow diagram

The Peng-Robinson equation of state (Peng & Robinson, 1976) with Boston-Mathias modification (PR-BM) (Mathias & Copeman, 1983) was used in the gas cycle, while the STEAMNBS method (Aspen plus®) in the steam cycle to predict the fluid properties in each section, depending on its nature.

Pre-treatment section

In the pre-treatment section the stack gas is cooled in a direct contact cooler with water at 25 ° C to improve the

Respuestas, 25 (3), pp. 54-78, 2020, ISSN 0122-820X - E ISSN: 2422-5053

absorption efficiency at 40 ° C and 1-1.5 bar (see Figure 2). Likewise, a blower was used to take into account the pressure losses that occur throughout the entire process.

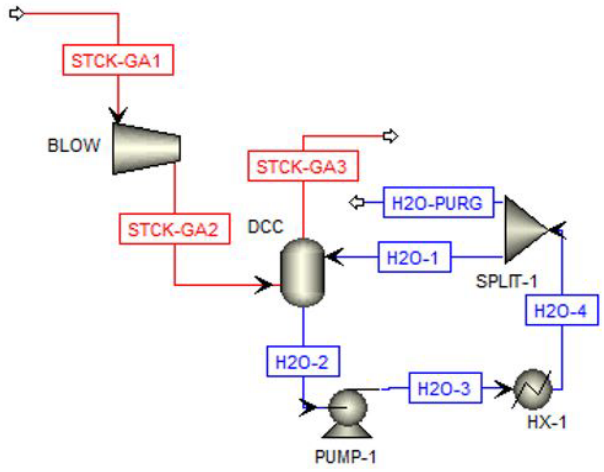

Figure 2. Pre-Treatment process diagram

Thermodynamic modelling

The thermodynamic and transport properties of the IL [Bmim][BF4] used in Aspen plus® regarding phase equilibrium for the CO2-MEA-H2O and CO2-IL-MEA-H2O systems are collected in Table 1 (Huang et al., 2014).

Table 1. IL properties

Property	Unit	Value
Molecular weight	-	226.02
Boiling temperature	K	632.3
Critical temperature	K	886.1
Critical pressure	bar	27.4
Critical volume	cm^3/mol	655.4
Acentric factor	-	0.5276
Critical compressibility factor	-	0.2434
CO_2 absorption enthalpy	kJ/mol	3.801

Physical solubility

The vapor-liquid equilibrium model was calculated with the equation 1. The vapour phase is modeled with the Soave-Redlich Kwong equation of state (Soave, 1972) (see documentation). The liquid phase is modeled with the NRTL model (C.-C. Chen & Evans, 1986; C. -C Chen, Britt, Boston, & Evans, 1982), whose binary interaction parameters for the MEA-H2O-CO2 system were taken from (Que & Chen, 2011; Zhang, Que, & Chen, 2011) and that with IL from (Huang et al., 2014).

$$y_i \widehat{\varphi}_i P = H_i x_i \gamma_i \qquad (1)$$

The Henry's constant dependence on temperature follows the equation 2, whose constants, for the binary pairs in which CO2 is involved (CO2-MEA-(Y. Liu, Zhang, & Watanasiri, 1999); CO2-H2O-(Yan & Chen, 2010); CO2-IL) (Huang et al., 2014), are summarized in Table 2.

$$\ln H_{ij} = C_1 + \frac{C_2}{T} + C_3 \ln T + C_4 T \qquad (2)$$

Table 2. Henry constants (Huang et al., 2014). Pressure in Pa.

Constants	Binary pairs		
	CO_2-MEA	CO_2-H_2O	CO_2-IL
C_1	80.452	100.65	43.7
C_2	-2934.6	-6147.7	10864
C_3	-11.6	-10.191	7.71
C_4	0.016	0	0.119
T[°C]	280-600	273-473	-

The following solubility data was used to validate the eNRTL thermodynamic model: the CO2 partial pressure was compared to different solvent loadings in aqueous solution with MEA; the total pressure of the system CO2-[Bmim][BF4] as a function of CO2 concentration; the total pressure as a function of the temperature for the binary system H2O-[Bmim][BF4] at a fixed concentration; the total pressure as a function of the temperature for the ternary system H2O-[Bmim][BF4]-MEA at a fixed concentration and at the CO2-MEA-H2O-IL system.

The data used for the validation of physical properties for both MEA and IL based solvent are given on Table 5. The root-mean-square deviation (RMSD) was used as a validation parameter (Equation 3).

$$RMSD = \sqrt{\frac{\sum_{i}^{N} (F(x_{i\exp}) - F(x_{i\mathrm{model}}))^2}{N}} \qquad (3)$$

Table 4. VLE experimental data

System	T [K]	P [kPa]	Source
CO_2-MEA-H_2O*	40-120	40-120**	(Aronu et al., 2011)
CO_2-[Bmim][BF_4]	313	1120-5530	(Lei et al., 2012)
H_2O-[Bmim][BF_4]	313-374	7.5-101.	(Huang et al., 2014)
H_2O-[Bmim][BF_4]-MEA	316-380	7.2-100.1	(Huang et al., 2014)

30%MEA concentration and loading from 0-0.6. ** CO2 partial pressure

Table 5. Physical properties experimental data

Property	MEA based			IL-based	Source	
	T[°C]	%MEA	Loading	T[K]	MEA based	IL-based
Heat capacity [kJ/kg•K]				190-370	(Weiland, Dingman, & Cronin, 1997)	(Paulechka, Blokhin, & Kabo, 2015)
Density [g/cm^3]	25	10-40	0-0.05	293-323	(Weiland, Dingman, Cronin, & Browning, 1998)	(Sanmamed, González-Salgado, Troncoso, Cerdeiriña, & Romaní, 2007)
Viscosity [mPa•s]				278-373		(Salgado et al., 2014)
Superficial Tension [mN/m]	30	10-30	0-0.722	284-351	(Fu, Xu, Wang, & Chen, 2012)	(Klomfar, Součková, & Pátek, 2010)
Thermal conductivity [W/m•K]	-	-	-	300-390		

The stack gas leaving the pre-treatment section enters the absorber, (Figure 3) where 90% of the CO2 in it is absorbed when contacted counter-currently with the solvent and wherein the reaction occurs between CO2 and the MEA contained in the lean solvent. The CO2 rich solvent that leaves the absorber bottom is pressurized at 2 bar and heated to 107°C by passing through a pump and heat exchanger, respectively, before to the regenerator's intake. In the regenerator, the compounds formed in the absorber are released through the application of heat, emitting a CO2 concentrated stream at the top and, from the bottoms, a regenerated solvent stream at a temperature of 125°C and 1.8 bar. The regenerator's top stream (CO2 >95% weight) is liquefied using compression to a pressure of 150 bar, so it can be easily transported to its final disposal; the solvent regenerated stream is recycled to the top of the absorber. The water and solvent make-up streams are introduced to overcome the losses that occur from their components in the top streams that leave the absorber and stripper.

"CALCULATOR" and "BALANCE" blocks to meet the streams or equipment specifications as well as the overall material balance. These are listed below.

"DESIGN SPEC" blocks

• The required water flow was calculated for the stack gas temperature, entering the absorber at 40°C.

• The desired capture level in the absorption column (for example, 90%) is achieved by manipulating the lean solvent flow that enters it.

• The required regeneration energy in the stripper is determined in such a way that the solvent leaving the column's bottom has the same CO2 loading as the lean solvent loading user-specified.

CALCULATOR" blocks: Stripper bottoms' flow is initially entered; this is recalculated once the lean solvent flow to achieve the desired capture level is obtained.

"BALANCE" blocks: Water and MEA balances were used to calculate water and MEA make-up streams, respectively.

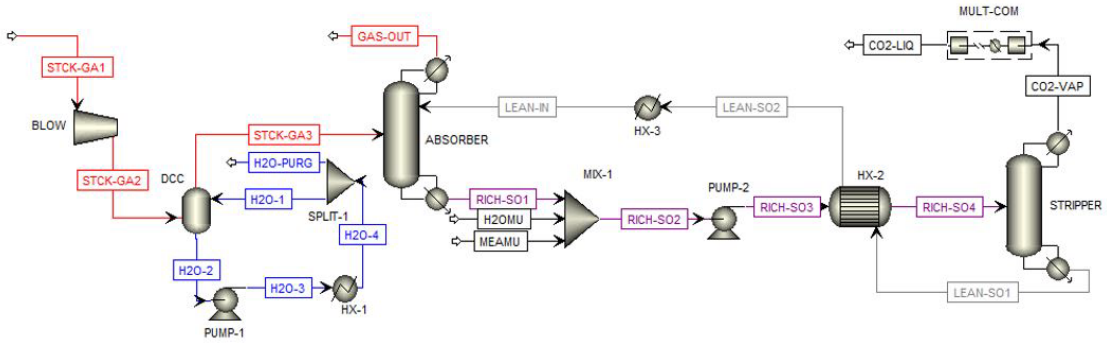

Figure 3. CO2 capture process flow diagram

Chemical reactions

CO2 is mainly soluble in the MEA-H2O solvent through a series of chemical equilibrium reactions shown below. The set of reactions that occur in the respective process columns are both equilibrium and kinetic type. These are shown in Table 6. Equation 4 models the equilibrium reactions, while Equation 5 the kinetic ones. The parameters of these reactions are shown in Table 7 (Zacchello et al., 2017), (Luo, 2016).

$$\ln K = A + \frac{B}{T} + C \ln T + DT \qquad (4)$$

$$r = k \exp(-\frac{E}{RT}) \prod_{i}^{N} C_i \qquad (5)$$

Table 6. CO2 Absorption reactions with MEA (Luo, 2016)

N	Reaction name	Stoichiometry
1	Water dissociation	$2H_2O \leftrightarrow H_3O^+ + OH^-$
2	Amine protonation	$MEAH^+ + H_2O \leftrightarrow MEA + H_3O^+$
3	CO_2 second dissociation	$HCO_3^- + H_2O \leftrightarrow CO_3^{2-} + H_3O^+$
4	CO_2 first dissociation	$CO_2 + OH^- \rightarrow HCO_3^-$
5	First inverted CO_2 dissociation	$HCO_3^- \rightarrow CO_2 + OH^-$
6	MEA-CO_2 reaction (absorption)	$MEA + CO_2 + H_2O \rightarrow MEACOO^- + H^3O^+$
7	MEA-CO_2 reaction(regeneration)	$MEACOO^- + H^3O^+ \rightarrow MEA + CO_2 + H_2O$

Table 7. Parameters for reactions in PCC process (Zacchello et al., 2017)

Reaction	A	B	C	D
1	132.9	-134446	-22.5	0
2	216.1	12431.7	-35.5	0
3	-3.04	7008.36	0	-0.00314
Reaction		k		E [J/kmol]
4		4.3E+13		5.55E+7
5		2.4E+17		1.23E+8
6		9.8E+10		4.13E+7
7		3.2E+19		6.55E+7

Respuestas, 25 (3), pp. 54-78, 2020, ISSN 0122-820X - E ISSN: 2422-5053

Scale-up

The CO2 capture plant needs to be scaled to meet the gas flow requirements of the 300MWe thermoelectric plant. This process is carried out maintaining the following constant:

- The capture level remains at 90%
- The solvent MEA concentration is 30%weight
- Operating pressures are 1 and 2 bar for the absorption and stripper columns, respectively

The design of the absorption and stripper columns implies the use of an adequate pressure drop value of 42 mm of water (Sinnot, 2005) thus an optimal gas-liquid distribution can be achieved. to estimate the columns diameters, as follows:

The solvent flow (F_{Lean}) through the columns was estimated by Equation 6 where the gas flow to be processed, gas density, liquid density, and viscosity are known values; likewise, a lean and rich solvent loading of 0.3 and 0.5 were assumed, respectively (Agbonghae, Hughes, Ingham, Ma, & Pourkashanian, 2014). Subsequently, the FLV flow parameter was calculated and k4, the modified gas load, is read from a pressure drop generalised correlation graph (Sinnot, 2005) assuming the mentioned pressure drop value Equation 7). Finally, the column cross sectional area is computed by Equation 8, where both the factor and length column's packing are required.

$$F_{Lean} = \frac{F_{Flue} x_{CO_2} \psi_{CO_2}}{100(\alpha_{Rich} - \alpha_{Lean})} \left[\frac{M_{MEA}}{44.009} \left(1 + \frac{1 - \omega_{MEA}}{\omega_{MEA}}\right) + \alpha_{Lean} \right] \qquad (6)$$

$$F_{LV} = \frac{L_W}{V_W} \sqrt{\frac{\rho_V}{d_L}} \qquad (7)$$

$$k_4 = \frac{13.1 \cdot V_W \cdot F_p \cdot \left(\mu_L / \rho_L\right)^{0.1}}{\rho_V (\rho_L - \rho_V)} \qquad (8)$$

Where F_{Lean} is the solvent flow; F_{flue} is the gas flow; F_{LV} is the flow parameter, L_w and V_w are the liquid and gas flows, respectively; x_{CO2} is the gas flow CO2 mass fraction; ΨCO2 is the specified capture level; α_{lean} and α_{rich} are CO2 solvent loading in the lean and rich solvent, respectively; M_{MEA} is the MEA molecular weight; ω_{MEA} is the MEA mass fraction; ρV and ρL are the vapour and liquid densities, respectively; k_4 is the modified gas load; μL the liquid viscosity and Fp the packing factor.

Economic section

The total equipment cost for the NGCC process was determined based on recognized vendors and literature data (DECARBit, 2011; DOE/NETL, 2007). For the PCC process, an economic technique, the cost module technique (CMT) was used. (Lemmens, 2016) found that the cost module technique presents deviations of -20% to +30% of the real cost. The CMT calculates the equipment cost in relation to their previous one on certain base conditions. In addition, deviation factors are introduced to take into account conditions different from standard ones.

Results and discussion

Vapour-liquid equilibrium and thermodynamic properties

The model adequately predicts the experimental vapour-liquid equilibrium data (Figure 4). The highest RMSD was found for the CO2-MEA-H2O system data, with a greater deviation as the system temperature increases (Table 8S, supporting material).

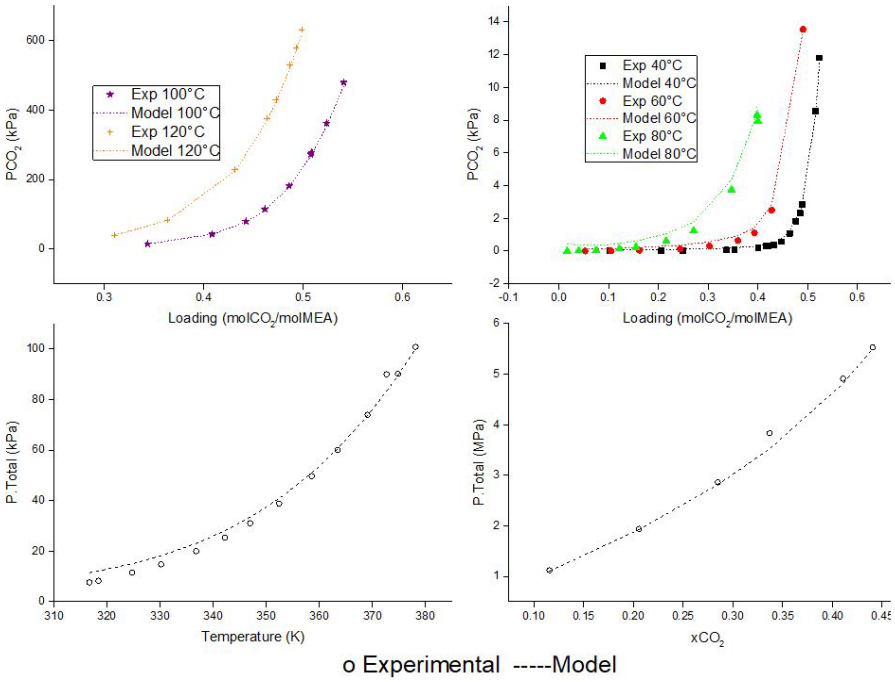

Figure 4. CO2 partial pressure as function of solvent loading, 30%MEA concentration at: a) 40,60,80°C, b)100,120°C. c) Pressure as function of CO2 concentration in the system CO2-[Bmim][BF4]. D) Pressure as function of temperature in the system H2O (1)-[Bmim][Bmim][BF4] (2)-MEA (3) with x1=0.6294, x2=0.0705

The model also predicts the physical properties experimental data accurately (see Figure 5 and Figure 6). The properties with the highest deviations are the surface tension and the heat capacity for the system based on MEA and IL, respectively (Table 9S, supporting material).

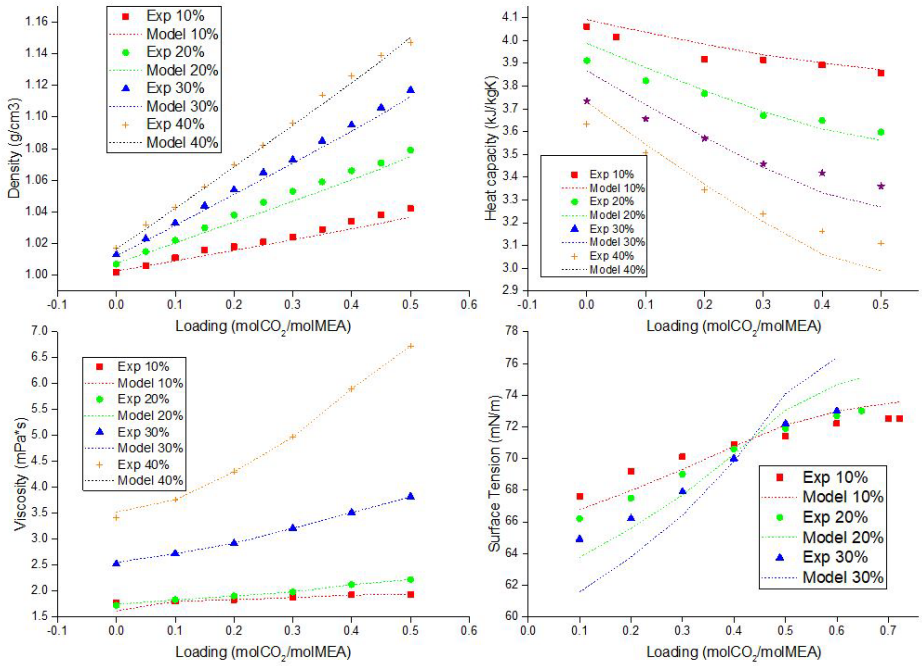

Figure 5. a) Density, b) Heat capacity, c) Viscosity, d) superficial tension as function of solvent loading and different MEA concentrations

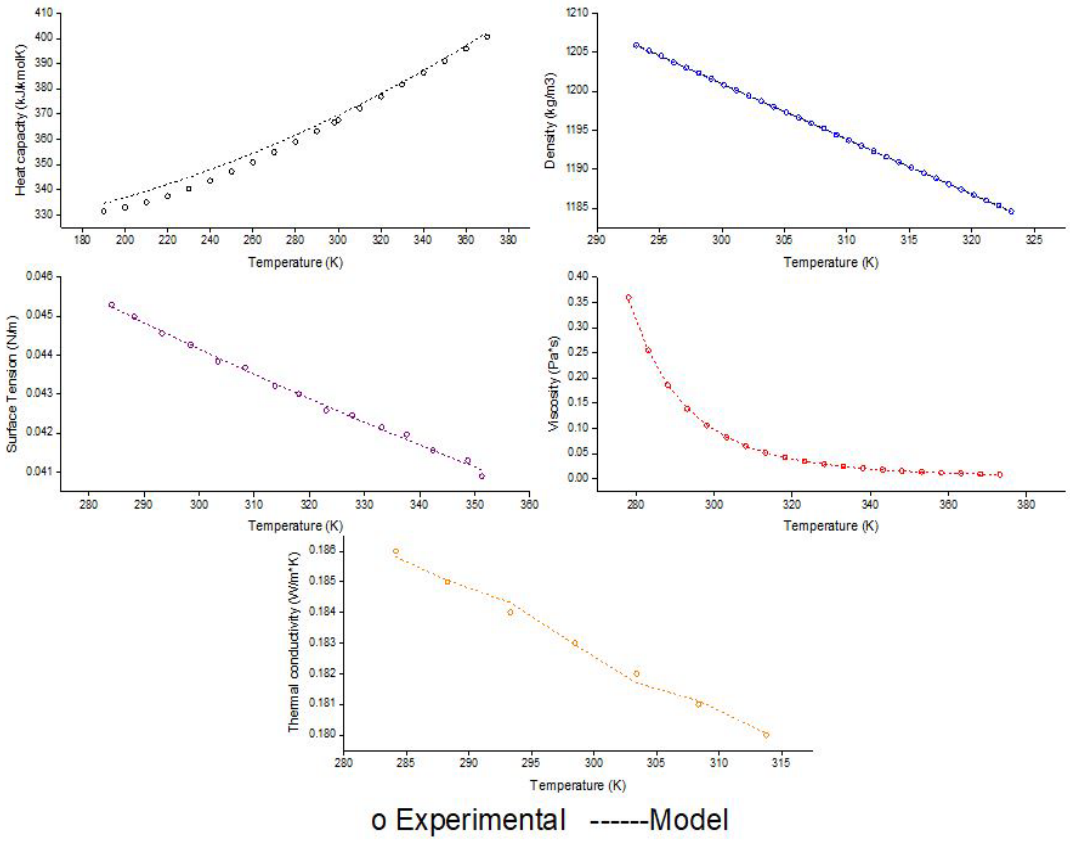

Figure 6. a) Heat capacity, b) density, c) viscosity, d) superficial tension, e) thermal conductivity as function of temperature for the ionic liquid [Bmim][BF4]

NGCC plant

According to the results obtained for the gas and steam cycles (Table 8), it can be stated that the model adequately predicts the available comparative parameters in an acceptable engineering error range; the highest deviation found was 18.67% regarding the stack gas temperature leaving the gas turbine.

Table 8. NGCC results and validation

Parameter	Aspen Plus	ISAGEN	Deviation [%]
Air Flow [kg/s]	464.76	-	-
Cooling Flow [kg/s]	232.38	-	-
Combustor temperature[°C]	1696.3	-	-
Flue gas temperature [°C]	628.96	530	18.67
Water Flow [kg/s]	66.11	-	-
HPS temperature[°C]	602.5	516	16.76
HPS pressure [bar]	87	87	0
LPS temperature[°C]	270.3	293	7.75
LPS pressure [bar]	10.6	10.6	0
Net power plant [MW]	300	300	0

Stack gas properties

The stack gas stream operational conditions after HRSG outlet and after the pre-treatment section are shown in Table 9. It is evident that after the pre-treatment section the water in the stack gas was partially condensed, therefore decreasing its concentration. At this point, the temperature was adjusted to 40°C at the exit.

Table 9. Flue gas properties right before exiting the NGCC process and entering the PCC

Parameter	After HRSG	After Pre-Treatment
Effluent Flow gas[kg/s]	476.382	468.234
Temperature [°C]	178	40
Pressure[kPa]	101.3	140
Composition [%weight]		
H_2O	5.010	3.350
N_2	74.719	76.048
O_2	13.487	13.743
CO_2	6.413	6.857
NOx	0.322	1e-7

CO2 capture plant

Model validation

A reference model for the simulations of CO2 absorption plant for a binary MEA-H2O mixture as a solvent was taken

Respuestas, 25 (3), pp. 54-78, 2020, ISSN 0122-820X - E ISSN: 2422-5053

from (Luo & Wang, 2017). The CO2 absorption model was simulated in Aspen Plus®, using a RADFRAC model based on mass and energy transfer rate correlations for the absorber and stripper columns. The results shown in Table 10 confirm that the developed model adequately predicts the conditions of the CO2 capture process with respect to that reported by (Luo & Wang, 2017). The only parameter that was significantly underestimated was the solvent flow necessary to achieve 90% capture, which was 23.63% lower than reported.

Table 10. comparative parameters of the Aspen Plus PCC

Parameter	This Work	(Luo & Wang, 2017)
Absorber Diameter[m]	13.11	14
Absorber packing height[m]	15	15
Stripper diameter[m]	5.89	6
Stripper packing height [m]	10	9.4
L/G [kg/kg]	1.958	1.58
Solvent flow [kg/s]	697.2	563.91
Lean solvent loading [molCO_2/molMEA]	0.3	0.303
Rich solvent loading [molCO_2/molMEA]	0.472	0.472
Specific duty [GJ/tonCO_2]	3.165	3.76

PCC: MEA e IL cases

Next to the validation, the ISAGEN NGCC-thermoelectric plant stack gas was treated in the CO2 capture process for two cases: with an aqueous solution of 30% MEA and with an optimum concentration of 5% IL, 30% MEA and 65 % water-the concentration of IL is justified in the sensitivity analysis of section 2.3.3, wherein is determined that this value requires the minimum amount of heat to regenerate the solvent-. The PCC process thermal and electrical requirements are found in Table 11. The thermal power for the PCC (IL) case decreased significantly respect to the case PCC (MEA) due to the lower regeneration energy required, while the electrical power, dependent on flow through equipment, varied only slightly. The regeneration energy decreased by 37.71% due to the lower IL enthalpy of absorption, compared with that of MEA (see Table 1). The compressors used to liquefy the CO2 represent the highest electrical power consumption, close to 72.62%. The power of this equipment, together with that of the pump and blower, represents a decrease in the net electric power once the NGCC and PCC processes are coupled.

Table 11. PCC process thermal and electrical requirements

Parameter		PCC(MEA)	PCC(IL)
Thermic Power[MWth]			
Regeneration energy	Boiler	136.404	83.96
	Condenser	50.113	
	Sensible heat	29.264	31.35
	Desorption heat	55.419	2.496
Lean solvent cooler		16.711	16.41
Effluent gas cooler		106.097	
Electric Power [MWe]			
Compression and cooling of CO_2		45.015	
Pumps		0.637	0.661
Blower		16.336	

The set-out case results for CO2 capture process are summarized in Table 12. It is observed that is required 4,279 GJ/tonCO2 of energy to achieve a capture level of 90%, which is a value in the range of those reported in the literature (e.g:(Canepa & Wang, 2015; Luo & Wang, 2017; Ma et al., 2017; Zacchello et al., 2017)), and it decreases to 2.9GJ/tonCO2 for the ionic liquid case.

The results once the NGCC and PCC processes were coupled are shown in Table 13. This was achieved by the processing of the stack gas, the extraction of the steam heading the steam turbines in the first process, and its introduction to the stripper's boiler.

Table 12. PCC performance results summary

Parameter	PCC(MEA)	PCC(IL)
Capture level [%]	90	
Effluent gas flow [kg/s]	468.234	
CO_2 in feed [%peso]	6.857	
Captured CO_2 [ton/year]	1005298	
Solvent concentration [%peso]	30	
Solvent flow[kg/s]	748.30	735.0
Lean solvent loading [molCO_2/mol MEA]	0.3	
Rich solvent loading [molCO_2/molMEA]	0.491	0.494
Regeneration energy [MWth]	136.40	83.96
Specific regeneration energy [GJ/tonCO_2]	4.279	2.9

In this case, there is no distinction between PCC (MEA) and PCC (IL). Although the thermal energy in the second process decreases due to the ionic liquid presence, the solvent flow, which affects electrical equipment, does not vary appreciably and therefore little decreases the process overall electrical power. The net power decreased from 300 MW for the NGCC to 238.011 MW for the NGCC-PCC coupled process; a decrease of 20.66%. The efficiency decreased from 49.733% to 39.45%, in a respective manner. The avoided carbon dioxide cost was \$82.77/tonCO_2.

Table 13. Simple and compound processes results summary

Parameter	NGCC	NGCC-PCC
Net power [MW]	300	238.01
Net efficiency [%HHV]	49.733	39.457
CO_2 emissions [tonCO_2/y]	$1.07x10^6$	$1.12x10^5$
CO_2 specific emissions [tonCO_2/MW]	3568.1	469.28
CO_2 captured [tonCO_2/year]	-	$1x10^6$
Avoided CO_2 [\$/tonCO_2]	-	82.77

Respuestas, 25 (3), pp. 54-78, 2020, ISSN 0122-820X - E ISSN: 2422-5053

Sensitivity analysis

MEA case

For the aqueous 30% (w/w) solvent, sensitivity parameters of the PCC process were varied to perceive how they affected the behaviour of others.

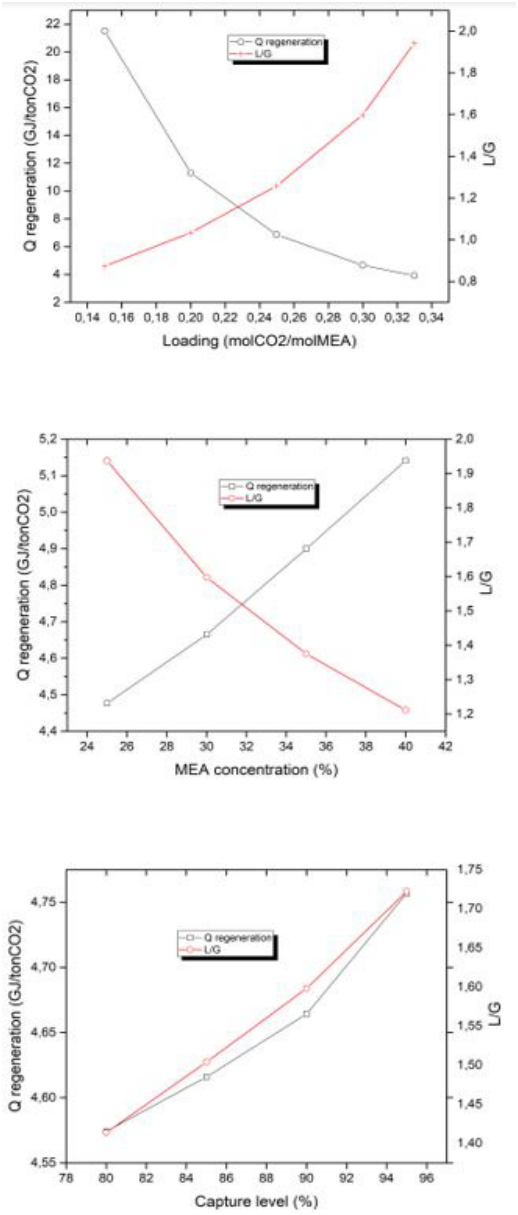

Figure 7. Regeneration energy and L/G as function of a) solvent loading at 30%MEA b) MEA solvent concentration at 0.3 mol/mol loading and c) plant capture level at a 30%MEA concentration and 0.3mol/mol loading.

Figure 7.a shows that the solvent flow increased proportionally with the CO2 loading since the concentration of CO2 in the liquid phase increases. On the other hand, the regeneration energy decreased with the increase of CO2 loading. Figure 7.b indicates that an increase of MEA solvent concentration produced an increment of regeneration energy and a decrement of solvent flow. Figure 7.c shows that both the regeneration energy and the solvent flow increase as

a higher capture level is specified. For example, the regeneration energy increases by 4% when going from a capture level of 80 to 95%. Similarly, the solvent flow rises 6.69% for the same change.

IL case

The sensitivity analysis was performed to analyze how the IL ([Bmim][BF4]) concentration in the solvent affected the regeneration energy and the solvent flow with a column reflux ratio constant throughout the entire concentration range, 30% (w/w) MEA and a CO2 loading of 0.3 mol/mol. In Figure 8 a decrement in both the regeneration energy and solvent flow over the entire concentration range was found. At 5% (w/w) IL the regeneration energy decreased by 37.71% (from 4.66 to 2.9 GJ/tonneCO2) and the liquid flow over gas flow (L/G) decreased only 1.77%. However, the L/G decreased to 9.3% at 40 % (W/W) [Bmim][BF4]). Conversely, the regeneration energy increases after 5%IL due to the increase in sensible heat-an increment in the bottoms temperature that exceeds the decrease in solvent flow at the stripper.

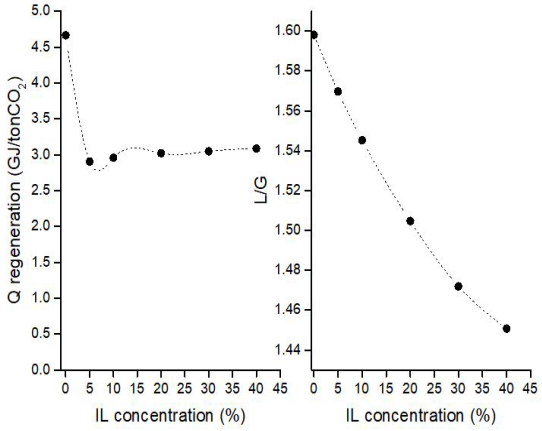

Figure 8. a) Regeneration energy, b) L/G as a function of IL concentration with solvent loading of 0.3 mol/mol

Subsequently, a concentration of 5% ionic liquid in the solvent (and 30% MEA) was selected as the optimum concentration and Q, L/G were analyzed as a function of CO2 loading. Figure 9 shows the variation of the regeneration energy (Q) and L/G at 30 % (w/w) MEA and 5 % (w/w) [Bmim][BF4]. Both the regeneration energy and the L/G ratio decrease with the loading, although always with a lower value for the IL case. Clearly L/G only varies slightly.

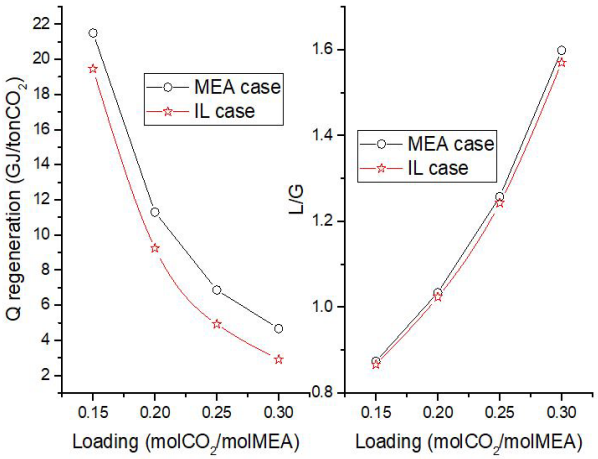

Figure 9. a) Regeneration energy (Q), b) L/G as a function of solvent loading

Respuestas, 25 (3), pp. 54-78, 2020, ISSN 0122-820X - E ISSN: 2422-5053

Economic results

The utilities used in the NGCC and PCC processes (Table 14) include the steam required to regenerate the solvent in the stripper, the electricity needed to operate pumps, cooling water and solvent cost-those of MEA an IL-. The obtained summary results are shown in Table 15 and Tables 10-19S.

Table 14. Utilities and raw materials

Natural gas [$/m^{3}]	0.42	(Turton, Bailie, Whiting, & Shaeiwitz, 2009)
HP steam [$/kg]	0.03	
Electricity [$/kWh]	0.093	(de Riva et al., 2017)
Water [$/m^{3}]	0.032	(Luo, 2016)
Refrigerant [$/GJ]	2.74	(Aspen Technology, 2013)
MEA[$/kg]	1.5	(ICIS Chemical Business, 2016)
IL[$/kg]	40	(Ramdin et al., 2012)

Capital cost

NGCC: The calculated total cost of equipment cost was $ 96,419 M. Of this value, the gas turbine represents 36.2%, the HRSG about 29% of the total cost. The steam turbine 21.1%, while the cooling system (pump-condenser system) the remaining 13.7%.

PCC (MEA): The choice of material and equipment types to be used was based on the considerations and recommendations on literature (IEAGHG, 2012). Stainless steel equipment was considered for MEA, a corrosive substance and carbon steel when the process fluid is water. The total equipment cost was 122.246 M$. The most expensive equipment was the absorber, which represents 46% of the total cost. The main process heat exchanger represents 20.42% of the total cost.

Table 15. Process economic results

Parameter	NGCC	MEA based	IL based
Net power [MW]	300	238.011	
Net efficiency [%HHV]	49.733	39.457	
CO_2 capture [tonCO_2/y]	-	1005298.22	
Avoided CO_2 [\$/tonCO_2]	-	82.77	
Equipment cost[M$]	96.419	122.246	
Direct+Indirect cost [M$]	184.661	280.114	
Total plant cost [M$]	212.36	322.131	
Manufacture cost [M$/year]	69.434	196.87	214.5

PCC (ILs): For this case, the optimum concentration of 5 % IL, found in the technical section, was used to size the equipment. The equipment dimensions are affected mainly by the solvent flow throughout the process and this did not decrease significantly for the selected concentration. A slight corrosion of the equipment, due to the lower presence of MEA may be present.

Manufacturing cost

The high-pressure steam represented 84% of the total utility cost for the MEA case. This is a clear confirmation that the CO2 regeneration energy in the stripper, measured in steam expenses, not only represents as a parameter the highest intensive energy consumption of the process, but the main process problem on the industry. For the IL [Bmim][BF4] case, the high-pressure steam represents 76.6% of the total utilities cost. However, the ionic liquid cost comes to represent an almost equivalent value.

As noted, the PCC manufacturing process cost for [Bmim][BF4] increased 8.22% implying that the decrement of high-pressure steam was not enough to compensate the high cost of the IL. (see Table 15).

On Figure 10 the solvent and the high-pressure steam costs as a function of the ionic liquid concentration is shown, in order to observe if the reduction in regeneration energy is worth the increment of the solvent cost.

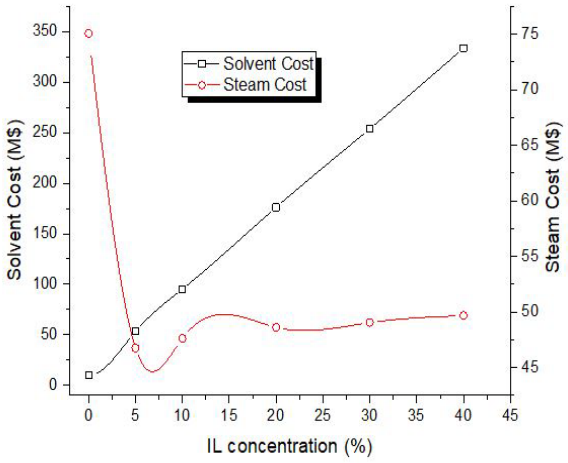

Figure 10. Solvent and steam cost as a function of IL concentration

It is observed that the steam cost was 37.71 % lower, the solvent cost 81.47% higher and the total cost (steam plus solvent) 17.67% higher at 5 % (w/w) [Bmim][BF4] when compared with only MEA in the solvent, meaning that, technically, a reduction of regeneration energy can be achieved by introducing an IL at expense of an economical infeasibility for the excessive increment in the solvent cost. This could be attributed to the IL cost assumed in this work ($40/kg IL).

Profitability analysis

In this section, an economic analysis of the NGCC process coupled to the PCC using as solvent H2O-30%(w/w) MEA and H2O-30%MEA-5%(w/w) IL was performed. The PCC case cannot be analyzed independently since, in this process, CO2 per se is not a defined value-added product. Therefore, the profitability analysis is carried out before and after coupling it to a PCC technology. This analysis is based on the completion of a non-discounted cumulative cash flow study. On Table 16 the conditions and/or assumptions for the profitability analysis are shown, which were taken from (Turton et al., 2009).

Table 16. Profitability analysis assumptions

Factor	Symbol	Description
Plant capital cost	CGR	Plant capital cost
Depreciation	dK	MACRS
Revenue	R	Net energy revenues
Manufacture costs	COMd	-
Land**	L	0.05CGR
Working capital**	WC	0.15CGR
Salvage	S	0
Plant time construction	n_{PC}	2
Depreciation time	n_D	5
Plant life time	n_{PL}	20
Tax rate	t	45%
Internal interest rate	i	12%

Figure 11 shows the cash flow along time for NGCC, NGCC-PCC(MEA) and NGCC-PCC (IL), suggesting that only for NGCC after 8.5 years (PBBP) the investment capital may be recovered with a net present value of 85.34M$ at the end of the 20 year.

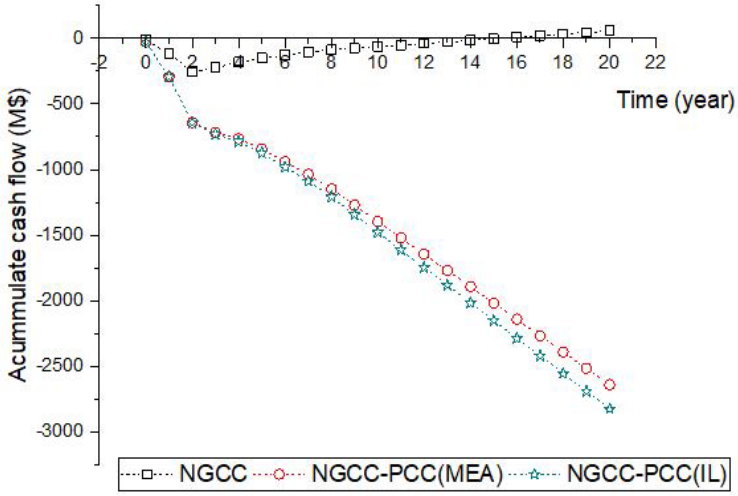

Figure 11. Cash flow throughout time for the studied processes

When the NGCC and PCC processes were coupled, electricity generation revenues decrease while the capital and manufacturing costs of both processes are combined. This, of course, causes the company to have a negative cash flow in the entire analyzed time range. This is also observed in Figure 11.

The analysis suggests that NGCC-PCC processes once coupled-either based on MEA or IL- were economically unfeasible, since the latter process causes a burden on capital and operational cost without any type of benefits on the first, more than the environmental one of avoiding the CO2 to be emitted to the atmosphere, with an additional revenue reduction in the first one by the lower net electricity produced.

However, and despite the above mentioned, we proceeded to investigate how to increase the cash flow once the processes are coupled and obtain a net present value (NPV) equal to the isolated NGCC process. This is a rather complex optimization problem, which is beyond the scope of this paper, but it was done in a simplified manner by minimizing the square difference having as an objective function the accumulated cash flow at the end of year 20, adjusting the following parameters of the NGCC and PCC processes: capital cost (CGR), manufacturing cost (COMd) and revenues (R). The results are shown in Figure 12 and Table 20S.

The results suggest that for the NGCC-PCC optimized process (MEA or IL), the CGR shall be reduced by 53.58%, from 534.49 to 248.069M$, since a relatively equal cost of equipment was assumed for both cases. In this sense the COMd shall be decreased 65.73% and 67.67% for NGCC-PCC (MEA) and NGCC-PCC (IL), respectively with a variation of R from 41.93 to 116.36M$ (63.97%) and 41.93 to 117.16M$ (64.65%), in a respective manner.

Respuestas, 25 (3), pp. 54-78, 2020, ISSN 0122-820X - E ISSN: 2422-5053

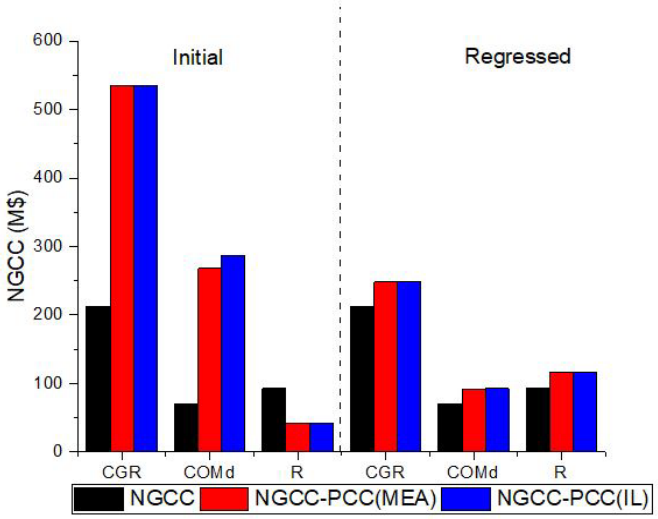

Figure 12. Column diagram of the process at their initial and optimized states

These results are in agree with reports (Metz, Davidson, Coninck, Loos, & Mayer, 2005) that indicate that for the NGCC-PCC compound process, the generation of electricity must increase between a 10-40% with respect to a plant that does not have a CO2 capture system, which explains the increase of the R for the PCC process.

Conclusions

In this work, the natural gas combined cycle (NGCC) process of the Colombian company ISAGEN and the carbon dioxide post-combustion capture process (PCC) were modeled in the Aspen Plus simulator. The feasibility of integrating the NGCC and PCC processes was analyzed through key parameters in the technical and economic studies carried out.

As a result, it was estimated that the 300MW Termocentro thermo-electric generation plant, which operates with the natural gas combined cycle technology (NGCC), has a payback time (PBP) of approximately 9.5 years and a net present value (NPV) of 57M$ at the end of year 20 of the performed case study.

The carbon dioxide capture plant once scaled to process the stack gas from the selected thermoelectric plant, has an L/G ratio of 1.6 and regeneration energy of 4.66GJ/tonneCO2 when 30% MEA is used as a solvent in the MEA-H2O system; these values are within the ranges reported in the literature. Once the ionic liquid [Bmim][BF4] was introduced into the solvent, i.e. the IL-MEA-H2O system with concentrations of 5% IL and 30% MEA, the results obtained indicate that the regeneration energy decreases to 2.9GJ/tonneCO2 (37.71%) and the L/G ratio 1.8%. This significant decrease in energy represents fewer utility costs for the plant in terms of steam in the stripper, not being the case for pump powers or heat exchange areas, parameters that are affected by solvent flows, which changed only negligible. These results agree with similar works in literature, which predict that introducing ionic liquids is technically favorable for PCC technologies.

Innovatively, this work studied the techno-economic viability of the implementation of ionic liquids in the capturing carbon dioxide process. The results show that neither the PCC process based on 30% MEA nor that based on ionic liquids at its optimum concentration of 5% are economically favorable if the PCC plant does not provide an additional economic benefit once it is coupled to the NGCC process.

To indicate a potential viability path for the PCC processes, an optimization problem was set out whose results suggest that for the PCC whether based on MEA or IL an extra income and a reduction in capital and manufacturing

costs shall be achieved for the NGCC-PCC compound process to have a net present value at least equal to that of the independent NGCC process.

Supplementary data

Supplementary data associated with this article can be found in the online version

Nomenclature

Symbol	Description
Cp	Heat capacity
H_{ij}	Henry constant
K	Equilibrium constant
L/G	Liquid Flow over gas flow
Q_{reg}	Regeneration energy
R	Ideal gas constant
T	Temperature
x_i	Molar fraction of component i in liquid mixture
ΨCO_2	CO_2 capture level
y_i	Molar fraction of component i in vapour mixture
αCO_2	CO_2 solvent loading

Symbols

Acronym	Description
CAPEX	Capital Expenditure
CCS	Carbon capture and storage
CGR	Capital Cost
CO_2	Carbon dioxide
COMd	Manufacture Cost
HHV	High heating value
IL	Ionic liquid
MEA	Monoethanolamine
NGCC	Natural gas combined cycle
NPV	Net present value
OPEX	Operational Expenditure
PCC	Post combustion capture process
RMSD	Root mean squared deviation

References

[1] IPCC, “Mitigation of Climate Change - Working Group III Contribution to the Fifth Assessment Report of the Intergovernmental Panel on Climate Change”, *IPCC*, 2014. doi.org/10.1017/CBO9781107415416.

[2] A. Kijewska and A. Bluszcz, "Analysis of greenhouse gas emissions in the European Union member states with the use of an agglomeration algorithm", *Journal of Sustainable Mining*, vol. 15, no. 4, pp. 133-142, 2016. doi.org/10.1016/J.JSM.2017.02.001.

[3] O. de Q. F. Araújo and de J. L. Medeiros, "Carbon capture and storage technologies: present scenario and drivers of innovation", *Current Opinion in Chemical Engineering*, vol. 17, pp. 22-34, 2017. doi.org/10.1016/J.COCHE.2017.05.004.

[4] L. Liu, J. Zhao, S. Deng and Q. An, "A technical and economic study on solar-assisted ammonia-based post-combustion CO2 capture of power plant", *Applied Thermal Engineering*, vol. 102, pp. 412-422, 2016. doi.org/10.1016/J.APPLTHERMALENG.2016.03.154.

[5] M. Ramdin, T. W. De Loos and T. J. H. Vlugt, "State-of-the-art of CO 2 capture with ionic liquids", *Industrial and Engineering Chemistry Research*, vol. 51, no. 24, pp. 8149-8177, 2012. doi.org/10.1021/ie3003705.

[6] D. Y. C. Leung, G. Caramanna, M. M. Maroto-Valer, "An overview of current status of carbon dioxide capture and storage technologies", *Renewable and Sustainable Energy Reviews*, vol. 39, pp. 426-443, 2014. doi.org/10.1016/J.RSER.2014.07.093.

[7] M. R. M. Abu-Zahra, L. H. J. Schneiders, J. P. M. Niederer, P. H. M. Feron and G. F Versteeg, "CO2 capture from power plants. Part I. A parametric study of the technical performance based on monoethanolamine", *International Journal of Greenhouse Gas Control*, vol. 1, no. 1, pp. 37-46, 2007. doi.org/10.1016/S1750-5836(06)00007-7

[8] R. Canepa and M. Wang, "Techno-economic analysis of a CO2capture plant integrated with a commercial scale combined cycle gas turbine (CCGT) power plant", *Applied Thermal Engineering*, vol. 74, pp. 10-19, 2015. doi.org/10.1016/j.applthermaleng.2014.01.014.

[9] X. Luo and M. Wang, "Improving Prediction Accuracy of a Rate-Based Model of an MEA-Based Carbon Capture Process for Large-Scale Commercial Deployment", *Engineering*, vol. 3, no. 2, pp. 232-243, 2017. doi.org/10.1016/J.ENG.2017.02.001.

[10] Agbonghae, E. O., Hughes, K. J., Ingham, D. B., Ma, L., & Pourkashanian, M, "Optimal Process Design of Commercial-Scale Amine-Based CO 2 Capture Plants". I*ndustrial & Engineering Chemistry Research*, vol. 53, no. 38, pp. 14815–14829, 2014. doi.org/10.1021/ie5023767.

[11] E., Gondal, S., Hessen, E. T., Haug-warberg, T., Hartono, A., Hoff, K. A., & Svendsen, H. F, "Solubility of CO 2 in 15, 30, 45 and 60 mass % MEA from 40 to 120 1 C and model representation using the extended UNIQUAC framework". *Chemical Engineering Science*, vol. 66, no. 24, pp. 6393–6406, 2011. doi.org/10.1016/j.ces.2011.08.042.

[12 Aspen Technology, "Aspen Physical Property System, Physical Property Models". *Burlington*, 2013

[13] Chen, C.-C., & Evans, L. B, "A local composition model for the excess Gibbs energy of aqueous electrolyte systems". *AIChE Journal*, vol. 32, no. 3, pp. 444–454, 1986. https://doi.org/10.1002/aic.690320311.

[14] Chen, C. -C, Britt, H. I., Boston, J. F., & Evans, L. B, "Local composition model for excess Gibbs energy of electrolyte systems. Part I: Single solvent, single completely dissociated electrolyte systems". *AIChE Journal*, vol. 28, no. 4, pp. 588–596, 1982. doi.org/10.1002/aic.690280410.

[15] Davis, J., & Rochelle, G, "Thermal degradation of monoethanolamine at stripper conditions". *Energy Procedia*, vol. 1, no. 1, pp. 327–333. doi.org/10.1016/j.egypro.2009.01.045.

[16] Riva, J., Suarez-Reyes, J., Moreno, D., Dïaz, I., Ferro, V., & Palomar, J, "Ionic liquids for post-combustion CO2capture by physical absorption: Thermodynamic, kinetic and process analysis". *International Journal of Greenhouse Gas Control*, vol. 61, pp. 61–70, 2017. doi.org/10.1016/j.ijggc.2017.03.019

[17] DECARBit, "Enabling advanced pre-combustion capture techniques and plants". DECARBit, 2011.

[18] DOE/NETL, "Cost and Performance Baseline for Fossil Energy Plants". *DOE/NETL*, 2007.

[19] Fu, D., Xu, Y., Wang, L., & Chen, L, "Experiments and model for the surface tension of carbonated monoethanolamine aqueous solutions". *Science China Chemistry*, vol. 55, no. 7, pp. 1467–1473, 2012. doi.org/10.1007/s11426-012-4641-7

[20] Guerrero Suarez, F., & Llano Camacho, F. (2003). "Gas natural en Colombia". *Scielo*, vol. 10, no. 87, pp. 115–146, 2003. Scielo.org.co/scielo.php?script=sci_arttext&pid=s0123-59232003000200006.

[21] Hasib-ur-Rahman, M., Siaj, M., & Larachi, F, "Ionic liquids for CO2 capture—Development and progress". *Chemical Engineering and Processing: Process Intensification*, vol. 49, no. 4, pp. 313–322, 2010. doi.org/10.1016/J.CEP.2010.03.008.

[22] Huang, Y., Zhang, X., Zhang, X., Dong, H., & Zhang, S, "Thermodynamic Modeling and Assessment of Ionic Liquid-Based CO 2 Capture Processes". *Industrial & Engineering Chemistry Research*, vol. 53, no. 29, pp. 11805–11817, 2014. doi.org/10.1021/ie501538e.

[23] ICIS Chemical Business, "Price and market trends: Europe ethanolamines stable to firm". *ICIS Chemical Business*, 2016.

[24] IEAGHG, "CO2 capture at gas fired power plants". *IEAGHG*, 2012.

[25] ISAGEN, "Isagen, Energía productiva. Central térmica termocentro". *ISAGEN*, 2018.

[26] Janković, B., Manić, N., Buchner, R., Płowaś-Korus, I., Pereiro, A. B., & Amado-González, E, "Dielectric properties and kinetic analysis of nonisothermal decomposition of ionic liquids derived from organic acid". *Thermochimica Acta*, vol. 672, pp. 43–52, 2019. doi.org/10.1016/J.TCA.2018.12.013.

[27] Klomfar, J., Součková, M., & Pátek, J, "Surface tension measurements with validated accuracy for four 1-alkyl-3-methylimidazolium based ionic liquids". *The Journal of Chemical Thermodynamics*, vol. 42, no. 3, pp. 323–329, 2010. doi.org/10.1016/J.JCT.2009.09.007.

[28] Krzemień, A., Więckol-Ryk, A., Smoliński, A., Koteras, A., & Więcław-Solny, L, "Assessing the risk of corrosion in amine-based CO2 capture process". *Journal of Loss Prevention in the Process Industries*, vol. 43, pp. 189–197, 2016. doi.org/10.1016/J.JLP.2016.05.020.

[29] Lei, Z., Han, J., Zhang, B., Li, Q., Zhu, J., & Chen, B, "Solubility of CO 2in Binary Mixtures of Room-Temperature Ionic Liquids at High Pressures". *Journal of Chemical & Engineering Data*, vol. 57, no. 8, pp. 2153–2159, 2012. doi.org/10.1021/je300016q.

[30] Lemmens, S, "Cost Engineering Techniques and Their Applicability for Cost Estimation of Organic Rankine Cycle Systems". *MDPI*, vol. 485, no. 9, 2016. doi.org/10.3390/en9070485.

[31] Liu, Y., Zhang, L., & Watanasiri, S, "Representing Vapor−Liquid Equilibrium for an Aqueous MEA−CO 2System Using the Electrolyte Nonrandom-Two-Liquid Model". *Industrial & Engineering Chemistry Research*, vol. 38, no. 5, pp. 2080–2090, 1999. doi.org/10.1021/ie980600v.

[32] Luo, X, "The university of hull faculty of sciences and engineering phd thesis process modelling , simulation and optimisation of natural gas combined cycle power plant integrated with carbon capture". *Xiaobo Luo Supervisor: Professor Meihong Wang*, May. 2016.

[33] Ma, T., Wang, J., Du, Z., Abdeltawab, A. A., Al-Enizi, A. M., Chen, X., & Yu, G. (2017). "A process simulation study of CO2capture by ionic liquids". *International Journal of Greenhouse Gas Control*, bol. 58, pp. 223–231, 2017. doi.org/10.1016/j.ijggc.2017.01.017.

[34] Mathias, P. M., & Copeman, T. W, "Extension of the Peng-Robinson equation of state to complex mixtures: Evaluation of the various forms of the local composition concept". *Fluid Phase Equilibria*, vol.13, pp. 91–108, 1983. doi.org/10.1016/0378-3812(83)80084-3.

[35] Metz, B., Davidson, O., Coninck, H. de, Loos, M., & Mayer, L, "IPCC special report on carbon dioxide capture and storage. Intergovernmental Panel on Climate Change". C*ambridge University Press*, 2005.

[36] Paulechka, Y. U., Blokhin, A. V, & Kabo, G. J, "Evaluation of thermodynamic properties for non-crystallizable ionic liquids". *Thermochimica Acta*, vol. 604, pp. 122–128, 2015. doi.org/10.1016/J.TCA.2015.01.022.

[37] Peng, D.-Y., & Robinson, D. B. (1976). "A New Two-Constant Equation of State". *Industrial & Engineering Chemistry Fundamentals*, vol. 15, no. 1, pp. 59–64, 1976. doi.org/10.1021/i160057a011.

[38] Que, H., & Chen, C.-C, "Thermodynamic Modeling of the NH 3 –CO 2 –H 2 O System with Electrolyte NRTL Model". *Industrial & Engineering Chemistry Research*, vol. 50, no. 19, pp. 11406–11421, 2011. doi.org/10.1021/ie201276m.

[39] Salgado, J., Regueira, T., Lugo, L., Vijande, J., Fernández, J., & García, J, "Density and viscosity of three (2,2,2-trifluoroethanol + 1-butyl-3-methylimidazolium) ionic liquid binary systems". *The Journal of Chemical Thermodynamics*, vol. 70, pp. 101–110, 2014. doi.org/10.1016/J.JCT.2013.10.027.

[40] Sanmamed, Y. A., González-Salgado, D., Troncoso, J., Cerdeiriña, C. A., & Romaní, L, "Viscosity-induced errors in the density determination of room temperature ionic liquids using vibrating tube densitometry". *Fluid Phase Equilibria*, vol. 252, no. 1–2, pp. 96–102, 2007. doi.org/10.1016/j.fluid.2006.12.016.

[41] Sinnot, R. K."Chemical Engineering Design. Elsevier". 2005

[42] Soave, G, "Equilibrium constants from a modified Redlich-Kwong equation of state". *Chemical Engineering Science*, vol. 27, no. 6, pp. 1197–1203, 1972. doi.org/10.1016/0009-2509(72)80096-4.

[43] Turton, R., Bailie, R. C., Whiting, W. B., & Shaeiwitz, J. A, "Analysis, Synthesis, and Design of Chemical Processes (Third)". *Prentice Hall,* 2009.

[44] Weiland, R. H., Dingman, J. C., & Cronin, D. B. (1997). "Heat Capacity of Aqueous Monoethanolamine, Diethanolamine, N -Methyldiethanolamine, and N -Methyldiethanolamine-Based Blends with Carbon Dioxide". *Journal of Chemical & Engineering Data*, vol. 42, no. 5, pp. 1004–1006, 1997. doi.org/10.1021/je960314v.

[45] Weiland, R. H., Dingman, J. C., Cronin, D. B., & Browning, G. J, "Density and viscosity of some partially carbonated aqueous alkanolamine solutions and their blends". *Journal of Chemical and Engineering Data*, vol. 43, no. 3, pp. 378–382, 1998. doi.org/10.1021/je9702044.

[46] Yan, Y., & Chen, C. C, "Thermodynamic modeling of CO2solubility in aqueous solutions of NaCl and Na2SO4". *Journal of Supercritical Fluids*, vol. 55, no. 2, pp. 623–634, 2010. doi.org/10.1016/j.supflu.2010.09.039.

[47] Zacchello, B., Oko, E., Wang, M., & Fethi, A, "Process simulation and analysis of carbon capture with an aqueous mixture of ionic liquid and monoethanolamine solvent". *International Journal of Coal Science and Technology*, vol. 4, no. 1, pp. 25–32, 2017. doi.org/10.1007/s40789-016-0150-1.

[48] Zhang, Y., Chen, H., Chen, C. C., Plaza, J. M., Dugas, R., & Rochelle, G. T, "Rate-based process modeling study of CO2 Capture with aqueous monoethanolamine solution". Industrial and Engineering Chemistry Research, vol. 48, no. 20, pp. 9233–9246, 2009. doi.org/10.1021/ie900068k.

[49] Zhang, Y., Que, H., & Chen, C. C, "Thermodynamic modeling for CO2absorption in aqueous MEA solution with electrolyte NRTL model". *Fluid Phase Equilibria*, vol. 311, no. 1, pp. 67–75, 2011. doi.org/10.1016/j.fluid.2011.08.025.